31st Annual International Conference of the IEEE EMBS
Minneapolis, Minnesota, USA, September 2-6, 2009

Tracking Variable Number of Multiple Subcellular Structures in 3D

Quan Wen and Jean Gao

Abstract— **With the introduction of sensitive and fast electronic imaging devices and the development of biological methods to tag proteins of interest by green fluorescent proteins (GFP), it has now become critical to develop automatic quantitative data analysis tools to study the live cell dynamics at subcellular level. In this paper, a sequential Monte Carlo (SMC) method to track variable number of multiple 3D subcellular structures is proposed. First, multiple subcellular structures are represented by a joint state. Then the distribution of the dimension changing joint state is sampled efficiently by the reverse jump Markov chain Monte Carlo (RJMCMC) method designed with update move, identity switch move, disappearing move, and appearing move. The experimental results show that the proposed method can successfully track multiple 3D subcellular structures with different motion modalities such as object appearing and disappearing.**

I. Introduction

With the wide application of bio-markers in biomedical experiments, it has now become critical to develop automatic quantitative data analysis tools for the studying of live cell dynamics at subcellular level. However, there lacks a general computational methodology on how to represent, track, and model the motility of subcellular structures to meet the essential research needs arising from the biology research community.

The technical challenges for subcellular structure mobility analysis come from: (1) variable object size; (2) changing number of objects; (3) large shape deformation; (4) close-neighbored objects; (5) diverse motion modalities; and (6) high noise. The commonly developed object tracking techniques can not be directly applied here. For instance, conventional template-based feature matching methods are limited for tacking non-deformable and sparsely-neighbored objects, and the curve/surface evolution based tracking methods are susceptible to noise and inter-frame object displacement [1]. Multiple-hypothesis tracking (MHT) [2] based methods need to handle exponential computation complexity, and joint probabilistic data association (JPDA) [3] methods face the problem of combinatorial complexity. Furthermore, there are several applications of RJMCMC [4] method to track variable number of multiple objects [5], [6]. However, the assumption that object will appear/disappear in certain fixed regions of the image scene is not applicable to generic subcellular image sequences.

Q. Wen is with the School of Computer Science and Engineering, University of Electronic Science and Technology of China, Chengdu, Sichuan, China quanwen@uestc.edu.cn

J. Gao is with the Department of Computer Science and Engineering, The University of Texas at Arlington, Arlington, TX 76019 gao@cse.uta.edu

To overcome the deficiencies of the current methods for multiple interacting object tracking, we present a tracking framework based on SMC method and approximate the joint state distribution at different time using RJMCMC sampling method. The background state is included into the joint state instead of using Markov random field (MRF) [6] to prevent the tracked objects being attracted to the high likelihood location. Furthermore, the restriction on the location of object appearing or disappearing is removed by the marker residual volume based appearing model. Experiment results on real confocal videos show that our method can track multiple 3D subcellular structures successfully.

The rest of this paper is organized as follows. The detection and representation of 3D subcellular structure are described in Section II. In Section III, we represent the variable number of multiple 3D subcellular structures by a joint state. The RJMCMC sampling method is detailed in Section IV, with the introduction of the 3D marker residual volume guided object appearing model in Section V and the observation mode in Section VI. Finally, the summary of the whole algorithm, experimental results, and conclusions are presented in Section VII, Section VIII, and Section IX, respectively.

II. Automatic 3D Subcellular Structure Detection and Representation

The regional maxima of a 3D gray-scale reconstructive opening operation $\circledcirc_3$ on the image volume I_{3t} are used to detect the subcellular structures. The operation is as: $I_{3t} \circledcirc_{C_3} S_3 = I_{3t} \odot_{C_3} (I_{3t} \circ_3 S_3)$, where S_3 is the 3D structuring element, $\odot_3$ is the 3D gray scale reconstruction operation, $\circ_3$ is the 3D gray scale morphological opening, and C_3 is the 3D connectivity definition for $\odot_3$. Each of the regional maxima of $I_{3.t} \circledcirc_{C_3} S_3$ is dilated once to include more voxel information. The corresponding binary volume is called marker volume $M_{3.t}$. The examples of regional maxima and marker volume are shown in Fig. 1(b) and Fig. 1(c).

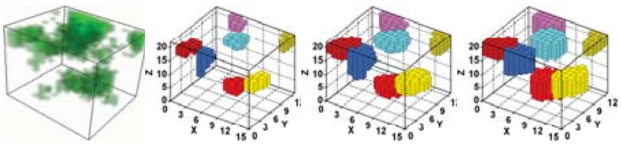

(a) (b) (c) (d)

Fig. 1. From regional maxima to state. (a) is the original volume. (b) is the regional maxima volume. (c) is the marker volume. (d) is OBV. The ratio between x, y, and z directions is x:y:z=5:5:1

For the oriented bounding volume (OBV) of each connected component (Fig. 1(d)), the length l, width w, height

h, and the corresponding rotation angles γ, β, and α [7] are used to represent each detected object as $\mathbf{X}_i = (x, y, z, l, w, h, \gamma, \beta, \alpha)^T$, where, (x, y, z) is the geometric center of the OBV.

III. Modeling Variable Number of 3D Subcellular Structures

We represent multiple 3D subcellular structures by a joint state $\mathbf{X}$, and denote it at time t as: $\mathbf{X}_t = \{\mathbf{X}_{t.i} | i \in n_t\}$, where n_t, with its cardinality $|n_t| \geq 1$, is the set of object identity number indicating which objects contribute to represent the joint state. The state of the object with ID i at time t is represented as $\mathbf{X}_{t.i} = (x_{t.i}, y_{t.i}, z_{t.i}, l_{t.i}, w_{t.i}, h_{t.i}, \gamma_{t.i}, \beta_{t.i}, \alpha_{t.i})^T$. The background with unchanging state is also treated as an object in our joint state model and represented as $\mathbf{X}_{t.0} = (x_0, y_0, z_0, l_0, w_0, h_0, \gamma_0, \beta_0, \alpha_0)^T$. It is the geometric information of the whole volume.

Given the state parameter vector $\mathbf{X}_t$ and object identity indicator set n_t, the joint distribution is denoted as $p(n_t, \mathbf{X}_{n_t})$. We factorize the state transition density function $p(n_t, \mathbf{X}_{n_t} | n_{t-1}, \mathbf{X}_{n_{t-1}})$ as $p(n_t, \mathbf{X}_{n_t} | n_{t-1}, \mathbf{X}_{n_{t-1}}) = p(\mathbf{X}_{n_t} | n_t, n_{t-1}, \mathbf{X}_{n_{t-1}}) \times p(n_t | n_{t-1}, \mathbf{X}_{n_{t-1}})$. Although the collision between 3D subcellular structures can happen in real, we treat such effects as the noise in the system equation and assume the independence between the individual states of each object. Thus $p(\mathbf{X}_{n_t} | n_t, n_{t-1}, \mathbf{X}_{n_{t-1}})$ can be further factorized as:

$$p(\mathbf{X}_{n_t} | n_t, n_{t-1}, \mathbf{X}_{n_{t-1}}) \triangleq \prod_{i \in \mathcal{S}_t} p(\mathbf{X}_{n_t.i} | \mathbf{X}_{(n_{t-1}).i}) \prod_{j \in \mathcal{B}_t} p(\mathbf{X}_{n_t.j}), \quad (1)$$

where $\mathcal{S}_t = n_t \cap n_{t-1}$ is the set of objects at time $t-1$ that remain at time t, $\mathcal{B}_t = n_t \setminus n_{t-1}$ is the set of new objects that are not in set n_{t-1}. Probability distribution $p(\mathbf{X}_{n_t.j})$ will be discussed in Section IV.

IV. RJMCMC Method for Sample Generation

The acceptance ratio of RJMCMC method is calculated as :

$$\alpha(n_t, \mathbf{X}_{n_t}; n'_t, \mathbf{X}'_{n_t}) = \frac{p(\mathbf{Z}_t | n'_t, \mathbf{X}'_{n_t}) p(n'_t, \mathbf{X}'_{n_t} | \mathbf{Z}_{1:t-1}) p_{m'} \times}{p(\mathbf{Z}_t | n_t, \mathbf{X}_{n_t}) p(n_t, \mathbf{X}_{n_t} | \mathbf{Z}_{1:t-1}) p_m \times} \frac{q_{m'}(\mathbf{U}; n'_t, \mathbf{X}'_{n_t})}{q_m(\mathbf{U}'; n_t, \mathbf{X}_{n_t})} \left| \frac{\partial(\mathbf{X}'_{n_t}, \mathbf{U}')}{\partial(\mathbf{X}_{n_t}, \mathbf{U})} \right|, \quad (2)$$

where $\mathbf{U}$ and $\mathbf{U}'$ are the auxiliary random variable vectors to guaranty that the mapping from $(\mathbf{X}_{n_t}, \mathbf{U})$ to $(\mathbf{X}'_{n_t}, \mathbf{U}')$ is a one-to-one mapping. p_m is the move specified probability and q_m is the proposal function for $\mathbf{U}$, where m, $m \in \{u, s, d, a\}$, with u, s, d, and a corresponding to update move, identity swap move, disappear move, and appear move, respectively. The last term of Eq. (2) is the Jacobian of the one-to-one mapping from $(\mathbf{X}_{n_t}, \mathbf{U})$ to $(\mathbf{X}'_{n_t}, \mathbf{U}')$. In this paper, we design the RJMCMC moves in a way such that the Jacobian term is always equal to one.

The four moves designed for the 3D object tracking are update move, identity swap move, disappear move, and appear move.

1) Update Move: An object identity number i is uniformly selected from the current identification number set n_t, and random walk is applied to it. The update move proposal is:

$$q_u(n'_t, \mathbf{X}'_{n_t}; n_t, \mathbf{X}_{n_t}) = q_u(i) q_u(n'_t, \mathbf{X}'_{n_t}; n_t, \mathbf{X}_{n_t}, i), \quad (3)$$

where $q_u(i) = 1/|n_t|$ is the proposal distribution for selecting i, $i \in \{n_t \setminus 0\}$, $q_u(n'_t, \mathbf{X}'_{n_t};\ n_t,\ \mathbf{X}_{n_t}, i) = q_u(\mathbf{U})$, where $q_u(\mathbf{U})$ is a Gaussian distribution.

2) Identity Swap Move: Two objects i and j in the current object set n_t are uniformly selected and their identities are exchanged. The identity swap move proposal is:

$$q_s(n'_t, \mathbf{X}'_{n_t}; n_t, \mathbf{X}_{n_t}) = q_s(i, j) q_s(n'_t, \mathbf{X}'_{n_t}; n_t, \mathbf{X}_{n_t}, i, j), \quad (4)$$

where $q_s(i, j) = 1/\binom{|n_t|}{2}$ is the proposal distribution for selecting the pair (i, j), and $q_s(n'_t, \mathbf{X}'_{n_t}; n_t, \mathbf{X}_{n_t}, i, j) = 1$.

3) Disappear Move: An object with identity number i is uniformly selected from the current identification number set n_t and its individual state is deleted from the joint state. The disappear move proposal is:

$$q_d(n'_t, \mathbf{X}'_{n_t}; n_t, \mathbf{X}_{n_t}) = q_d(i) q_d(n'_t, \mathbf{X}'_{n_t}; n_t, \mathbf{X}_{n_t}, i), \quad (5)$$

where $q_d(i) = 1/|n_t|$ is the proposal distribution for selecting i, $i \in \{n_t \setminus 0\}$, with $|\cdot|$ as the set cardinality operator, and $q_d(n'_t, \mathbf{X}'_{n_t}; n_t, \mathbf{X}_{n_t}, i) = 1$.

4) Appear Move: An object with identity number i is uniformly selected from set $\{\mathcal{A}_t \cup \bar{n}_t \setminus n_t\}$, with $\bar{n}_t = \cup_{k=1}^{N} n_{t-1}^{(k)}$, where N is the number of samples at time $t-1$ and $\mathcal{A}_t$ is the possible new object set at time t. $\mathcal{A}_t$ is constructed by image processing techniques and will be discussed in Section V. The individual state of the identification number i is added to the joint state. The appear move proposal is:

$$q_a(n'_t, \mathbf{X}'_{n_t}; n_t, \mathbf{X}_{n_t}) = q_a(i) q_a(n'_t, \mathbf{X}'_{n_t}; n_t, \mathbf{X}_{n_t}, i), \quad (6)$$

with $q_a(i) = 1/|\mathcal{A}_t \cup \bar{n}_t \setminus n_t|$ as the proposal distribution for selecting i, $i \in \{\mathcal{A}_t \cup \bar{n}_t \setminus n_t\}$, $q_a(n'_t, \mathbf{X}'_{n_t};\ n_t, \mathbf{X}_{n_t}, i) = q_a(\mathbf{U})$, where $q_a(\mathbf{U})$ is the proposal of generating the state for the newly added object. The formulation of $q_a(\mathbf{U})$ will be presented in Section V.

Plugging the proposal of each move into Eq. 2, we get acceptance ratios as follows:

$$\alpha_u = \alpha_s = \frac{p(\mathbf{Z}_t | n'_t, \mathbf{X}'_{n_t}) p(n'_t, \mathbf{X}'_{n_t} | \mathbf{Z}_{1:t-1})}{p(\mathbf{Z}_t | n_t, \mathbf{X}_{n_t}) p(n_t, \mathbf{X}_{n_t} | \mathbf{Z}_{1:t-1})}, \quad (7)$$

$$\alpha_d = \frac{p(\mathbf{Z}_t | n'_t, \mathbf{X}'_{n_t}) p(n'_t, \mathbf{X}'_{n_t} | \mathbf{Z}_{1:t-1}) p_a q_a(i) q_a(\mathbf{U}')}{p(\mathbf{Z}_t | n_t, \mathbf{X}_{n_t}) p(n_t, \mathbf{X}_{n_t} | \mathbf{Z}_{1:t-1}) p_d q_d(i)}, \quad (8)$$

$$\alpha_a = \frac{p(\mathbf{Z}_t | n'_t, \mathbf{X}'_{n_t}) p(n'_t, \mathbf{X}'_{n_t} | \mathbf{Z}_{1:t-1}) p_d q_d(i)}{p(\mathbf{Z}_t | n_t, \mathbf{X}_{n_t}) p(n_t, \mathbf{X}_{n_t} | \mathbf{Z}_{1:t-1}) p_a q_a(i) q_a(\mathbf{U})}. \quad (9)$$

For the evaluation of $p(n_t, \mathbf{X}_{n_t} | \mathbf{Z}_{1:t-1})$, we use its mixture approximation as: $\hat{p}(n_t, \mathbf{X}_{n_t} | \mathbf{Z}_{1:t-1}) = \frac{1}{N} \sum_{k=1}^{N} p(n_t, \mathbf{X}_{n_t} | n_{t-1}^{(k)}, \mathbf{X}_{n_{t-1}}^{(k)})$, where $p(n_t, \mathbf{X}_{n_t} | n_{t-1}^{(k)}, \mathbf{X}_{n_{t-1}}^{(k)})$ is evaluated as $p(n_t, \mathbf{X}_{n_t} | n_{t-1}^{(k)}, \mathbf{X}_{n_{t-1}}^{(k)}) = p(n_t | n_{t-1}^{(k)}, \mathbf{X}_{n_{t-1}}^{(k)}) \prod_{j \in \mathcal{B}_t} p(\mathbf{X}_{n_t.j}) \times \prod_{i \in \mathcal{S}_t} p(\mathbf{X}_{n_t.i} | \mathbf{X}_{(n_{t-1}).i}^{(k)})$, with $\mathcal{B}_t = n_t \setminus n_{t-1}^{(k)}$, $\mathcal{S}_t = n_t \cap n_{t-1}^{(k)}$ as previously introduced in section III. There are two cases for object identification number j in $\mathcal{B}_t$, $j \in \mathcal{A}_t$ and $j \notin \mathcal{A}_t$. For the first case, $p(\mathbf{X}_{n_t.j}) = p_{new}$, with $j \in \mathcal{A}_t$. For the second case, $p(\mathbf{X}_{n_t.j})$ is defined to be $p(\mathbf{X}_{n_t.j}) \triangleq \sum_{i \in N_{t-1}^{(j)}} p(\mathbf{X}_{n_t.j} | \mathbf{X}_{n_{t-1}.j}^{(i)}) / |N_{t-1}^{(j)}|$, with

$N_{t-1}^{(j)} = \{i : j \in n_{t-1}^{(i)}\}$, the set of samples at time $t-1$ containing object j. $n_{t-1}^{(i)}$ is the object set for particle i at time $t-1$. $p(n_t|n_{t-1}^{(k)}, \mathbf{X}_{n_{t-1}}^{(k)})$ is defined to be equivalent for all n_t, $n_{t-1}^{(k)}$, and $\mathbf{X}_{n_{t-1}}^{(k)}$, since we assume the equal chance of each object set n_t.

V. 3D Marker Residual Volume-Guided Appearing Model

We apply the marker residual volume-guided appearing model to detect new object appearing. For a 3D volume $I_{3.t}$ at time t, its marker volume $M_{3.t}$ can be denoted as $M_{3.t} = \cup_{i=1}^{n} M_{3.t.i}$, where $M_{3.t.i}$ is the volume of the ith connected component. A new volume called marker residual volume $\mathbb{M}_{3.t}$ that predicts possible newly appearing objects is defined as: $\mathbb{M}_{3.t} = \{M_{3.t.i} : M_{3.t.i} \cap M_{3.(t-1)} = \emptyset, i = 1, \cdots, n\}$. An example of the marker volume and marker residual volume is illustrated in Fig. 2.

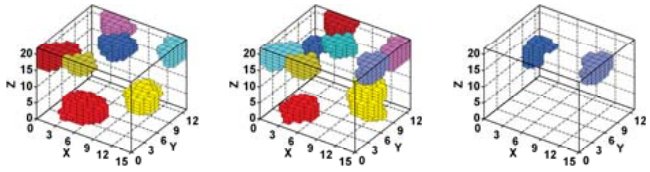

(a) (b) (c)

Fig. 2. Marker residual volume generation. (a) is marker volume $M_{3.8}$. (b) is marker volume $M_{3.9}$. (c) is marker residual volume $\mathbb{M}_{3.9}$. The ratio between x, y, and z directions is x:y:z=5:5:1

We treat each $\mathbb{M}_{3.t.i}$, as a possible new object and use it to construct the possible appearing object set $\mathcal{A}_t$. The aforementioned proposal function $q_a(\mathbf{U})$ for the new object is defined as follows:

$$q_a(\mathbf{U}) = \begin{cases} p(\mathbf{X}_{n_t.j}|\mathbb{M}_{3.t.j}), & \text{if} j \in \mathcal{A}_t \\ \sum_{i \in N_{t-1}^{(j)}} P(\mathbf{X}_{n_t.j}|\mathbf{X}_{(n_{t-1}).j}^{(i)}) / |N_{t-1}^{(j)}|, & \text{if} j \notin \mathcal{A}_t, \end{cases} \quad (10)$$

where $p(\mathbf{X}_{n_t.j}|\mathbb{M}_{3.t.j})$ generates the state by a Gaussian distribution center around the object in the image $\mathbb{M}_{3.t.j}$. $N_{t-1}^{(j)} = \{i : j \in n_{t-1}^{(i)}\}$ is the set of samples at time $t-1$ containing object j.

VI. 3D Observation Model

The joint observation model is defined as: $p(\mathbf{Z}_t|\mathbf{X}_t) = \prod_{i \in n_t} p(\mathbf{Z}_{t.i}|\mathbf{X}_{t.i})$. For the measurement of each individual object state $\mathbf{X}_{t.i}$, we use the intensity profile of the voxels inside its bounding volume to match with its reference $R_{t.i}$, which is obtained at the beginning of each object trajectory. Three properties are considered in our observation: (1) volume; (2) intensity mean; and (3) sorted sum-of-absolute-differences (SSAD). We define the observation model for each individual object as:

$$p(\mathbf{Z}_{t.i}|\mathbf{X}_{t.i}) = p(\mathbf{Z}_{t.i}^{v}|\mathbf{X}_{t.i}) p(\mathbf{Z}_{t.i}^{m}|\mathbf{X}_{t.i}) p(\mathbf{Z}_{t.i}^{d}|\mathbf{X}_{t.i}), \quad (11)$$

with $p(\mathbf{Z}_{t.i}^{v}|\mathbf{X}_{t.i})$, $p(\mathbf{Z}_{t.i}^{m}|\mathbf{X}_{t.i})$, and $p(\mathbf{Z}_{t.i}^{d}|\mathbf{X}_{t.i})$, for volume measurement, intensity mean, and SSAD, respectively, and

$$p(\mathbf{Z}_{t.i}^{v}|\mathbf{X}_{t.i}) \propto \exp\left(-\lambda_v \left(1 - \frac{\min(n,m)}{\max(n,m)}\right)^2\right), \quad (12)$$

$$p(\mathbf{Z}_{t.i}^{m}|\mathbf{X}_{t.i}) \propto \exp\left(-\lambda_m \left(1 - \frac{\min(I_{A_n}, I_{B_m})}{\max(I_{A_n}, I_{B_m})}\right)^2\right), \quad (13)$$

$$p(\mathbf{Z}_{t.i}^{d}|\mathbf{X}_{t.i}) \propto \exp\left(-\lambda_d \cdot (SSAD(A_n, B_m))^2\right), \quad (14)$$

with λ_v, λ_m, and λ_d are hyperparameters. Readers please refer to [8] for more details.

VII. Summary of the Algorithm

The algorithm for 3D subcellular structure tracking is summarized as follows:

1) Automatically detect the subcellular structures using marker residual volume. Estimate the state $\mathbf{X}_{0.i}$ of each individual subcellular structure, and combine them into $\mathbf{X}_0$. Sample the joint state $\mathbf{X}_0$ with N samples. Thus the initial distribution of $\mathbf{X}_0$ is approximated by $p(\mathbf{X}_0) \approx \{\mathbf{X}_0^{(s)}\}$, $s = 1, \ldots, N$. Set $t = 0$.
2) Set $t = t+1$. Draw a sample of $\mathbf{X}_t$ from the prediction density $\sum_{s=1}^{N} p(\mathbf{X}_t|\mathbf{X}_{t-1}^{(s)})/N$.
3) Apply RJMCMC method to draw N samples.
   a) Draw a sample w from the uniform distribution on $(0, 1)$.
   b) if $0 \le w < p_u$, apply update move.
   c) If $p_u \le w < p_u + p_s$, apply identity swap move.
   d) If $p_u + p_s \le w < p_u + p_s + p_d$, apply disappear move.
   e) If $p_u + p_s + p_d \le w$, apply appear move.
   f) Calculate the acceptance ratio $\alpha(\mathbf{X}_t, \mathbf{X}_t')$
   g) Draw a sample w' from the uniform distribution on $(0, 1)$. If $w' < \alpha(\mathbf{X}_t, \mathbf{X}_t')$, use $\mathbf{X}_t'$ as the new joint state; else use $\mathbf{X}_t$. Add the new state to the final sample set.
4) Go to step 2.

VIII. Experimental Results

The real 3D volume sequence data in our experiment has a total of 147 3D volumes, each with a size of $160 \times 140 \times 22$ voxels taken at an interval of 0.88 seconds. We use a portion of the 3D volume spanning 7.04 seconds to demonstrate our algorithm. Here the unit ratio of x, y, and z directions is set to be 5:5:1 for better 3D rendering effect instead of the original unit ratio 10:10:1.

One of the tracking results of our method is shown in Fig. 3. Among the tracked objects, object O1 is doing translational motion, and the others are doing Brownian motion. The movement of each subcellular structure is clearly demonstrated by its trajectory in Fig. 4 with different view angles.

For the quantitative evaluation of our algorithm, the average displacement error between the center of the tracked subcellular structure and that of the ground truth is shown in Fig. 5(a), with an average distance error of 0.9361 pixels of the x-y plane. Figure 5(b) shows the change of the number of objects during tracking process. "Truth" means the number of objects of the ground truth. "Correct" means that an object of the ground truth is correctly tracked. "Missing" object means that an object of the ground truth is not tracked. "Incorrect" means that a tracked object is not in the ground truth or not associated correctly. Our method successfully detected the changes of the number of the objects which were caused by object appearing and disappearing.

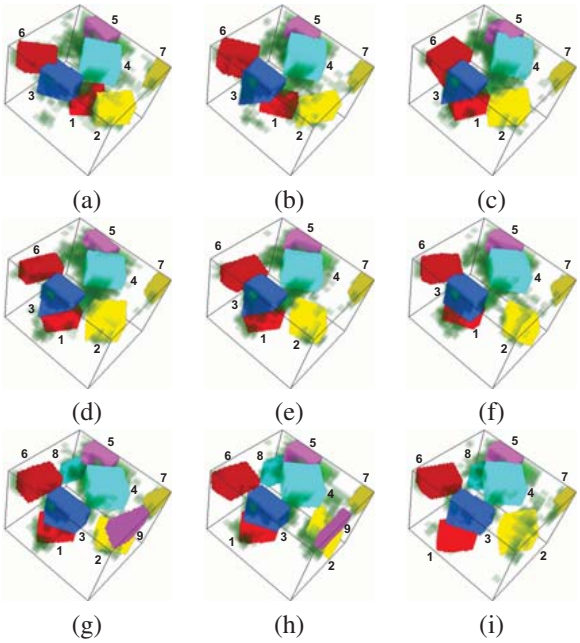

Fig. 3. Tracking results of subcellular structures embedded in the real volume sequence, with different subcellular structure indicated by different color. (a) to (i) are volumes at time 0 sec, 0.88 sec, 1.76 sec, 2.64 sec, 3.52 sec, 4.40 sec, 5.28 sec, 6.16 sec, and 7.04 sec. The ratio between x, y, and z direction is x:y:z=5:5:1

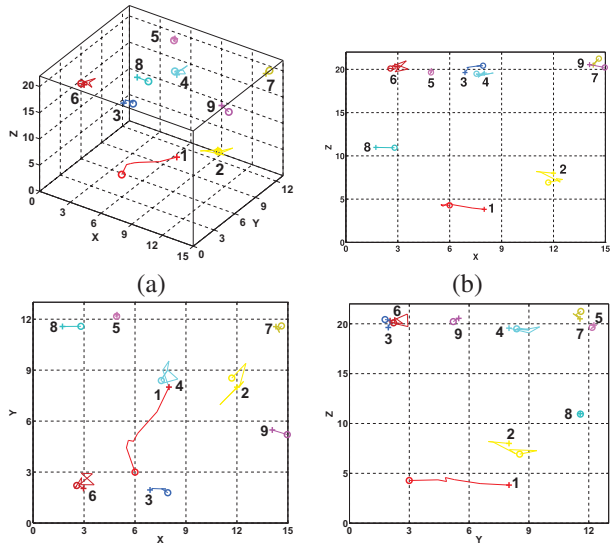

Fig. 4. Different views of the tracking trajectories. (a) is viewed with $azimuth = 34°$, $elevation = 32°$. (b) is viewed from y axis direction. (c) is viewed from z axis direction. (d) is viewed from x axis direction. The ratio between x, y, and z axes is x:y:z=5:5:1

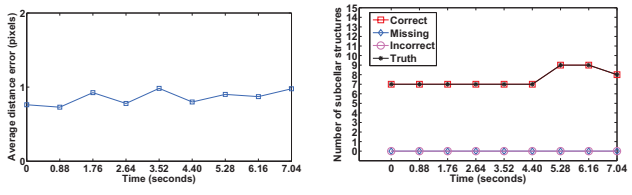

Fig. 5. (a) is the average distance error at each time by our method. (b) is the evaluation of the number of tracked object at each time by our method.

As for the parameters used in our method, the state transition density of $(x, y, z, l, w, h, \gamma, \beta, \alpha)^T$ was set to be a Gaussian distribution with zero mean vector and covariance matrix Σ_s, which is a 9×9 diagonal matrix with $\Sigma_{s11}=4$, $\Sigma_{s22}=4$, $\Sigma_{s33}=0.01$, $\Sigma_{s44}=0.5$, $\Sigma_{s55}=0.5$, $\Sigma_{s66}=0.05$, $\Sigma_{s77}=0.16$, $\Sigma_{s88}=0.16$, and $\Sigma_{s99}=2.5$. The random walk covariance matrix Σ_r is also a 9×9 diagonal matrix with $\Sigma_{r11}=1$, $\Sigma_{r22}=1$, $\Sigma_{r33}=0.0009$, $\Sigma_{r44}=0.01$, $\Sigma_{r55}=0.01$, $\Sigma_{r66}=0.0025$, $\Sigma_{r77}=0.01$, $\Sigma_{r88}=0.01$, and $\Sigma_{r99}=0.09$. p_u, p_s, p_d, and p_a are set to be 0.7, 0.1, 0.1, and 0.1, respectively, and the hyperparamers λ_v, λ_m, and λ_d, are set to be 7, 5, 0.4, respectively.

IX. Conclusions

In this paper, we presented a sequential Monte Carlo (SMC) framework for variable number of 3D multiple subcellular structure tracking. RJMCMC moves such as update move, identity switch move, disappearing move, and appearing move are applied to sample the dimension changing joint state of the multiple subcellular structures efficiently. Both the visual and quantitative experiment results show that our method can track different motion modalities such as Brownian and translational motions, and detect object appearing and disappearing correctly.

X. Acknowledgments

The authors are grateful for the support from National Science Foundation (NSF) under grant IIS-0546605.

References

[1] A. Dufour, V. Shinin, S. Tajbakhsh, N. Guillen-Aghion, J.-C. Olivo-Marin, and C. Zimmer, "Segmenting and tracking fluorescent cells in dynamic 3-D microscopy with coupled active surfaces," *IEEE Transactions on Image Processing*, vol. 14, no. 9, pp. 1396–1410, Sept. 2005.

[2] D. B. Ried, "An algorithm for tracking multiple targets," *IEEE Transactions on Automatic Control*, vol. AC-24, no. 6, pp. 843–854, Dec 1979.

[3] T. E. Fortmann, Y. Bar-Shalom, and M. Scheffe, "Sonar tracking of multiple targets using joint probabilistic data association," *IEEE Journal of Oceanic Engineering*, vol. OE-3, no. 3, pp. 173–184, July 1983.

[4] P. J. Green, "Reversible jump Markov chain Monte Carlo computation and Bayesian model determination," *Biometrika*, vol. 82, no. 4, pp. 711–732, 1995.

[5] K. Smith, D. Gatica-Perez, and J.-M. Odobez, "Using particles to track varying number of interacting people," in *Proceedings of IEEE Conference on Computer Vision and Pattern Recognition*, vol. 1, San Diego, CA USA, June 20-25 2005, pp. 962–969.

[6] Z. Khan, T. Balch, and F. Dellaet, "MCMC-based particle filtering for tracking a variable number of interacting targets," *IEEE Transaction on Pattern Analysis and Machine Intelligence*, vol. 27, no. 11, pp. 1805–1819, Nov. 2005.

[7] J. J. Craig, *Introduction to Robotics Mechanics and Control*, 2nd ed. Addison-Wesley Publishing Company, 1989.

[8] Q. Wen, J. Gao, and K. Luby-Phelps, "Multiple interacting subcellular structure tracking by sequential Monte Carlo method," in *IEEE International Conference on Bioinformatics and Biomedicine*, Fremont, CA USA, Nov 2007, pp. 437–442.